Comparison of techniques for dating of subsurface ice from Monlesi ice cave, Switzerland

Marc LUETSCHER,[1,2] David BOLIUS,[3] Margit SCHWIKOWSKI,[3] Ulrich SCHOTTERER,[4] Peter L. SMART[2]

[1]Swiss Institute for Speleology and Karstology (SISKA), CH-2301 La Chaux-de-Fonds, Switzerland
[2]School of Geographical Sciences, University of Bristol, Bristol BS8 1SS, UK
E-mail: marc.luetscher@bristol.ac.uk
[3]Paul Scherrer Institute, CH-5232 Villigen PSI, Switzerland
[4]Physics Institute, University of Bern, Sidlerstrasse 5, CH-3012 Bern, Switzerland

ABSTRACT. The presence of cave ice is documented in many karst regions but very little is known about the age range of this potential paleoclimate archive. This case study from the Monlesi ice cave, Swiss Jura Mountains, demonstrates that dating of cave ice is possible using a multi-parameter approach. Ice petrography, debris content and oxygen isotope composition have the potential for identification of annual growth layers, but require a continuous core from the ice deposits, limiting application of this approach. Furthermore, complete melting of ice accumulations from individual years may occur, causing amalgamation of several annual bands. Use of ^{3}H content of the ice and ^{14}C dating of organic debris present in the ice proved to be of limited utility, providing rather broad bounds for the actual age. Initial estimates based on ^{210}Pb analyses from clear ice samples gave results comparable to those from other methods. The most reliable techniques applied were the determination of ice turnover rates, and the dating of anthropogenic inclusions (a roof tile) in the ice. These suggest, respectively, that the base of the cave ice was a minimum of 120 and a maximum of 158 years old. Therefore, our data support the idea that mid-latitude and low-altitude subsurface ice accumulations result from modern deposition processes rather than from presence of Pleistocene relict ice.

INTRODUCTION

Mid-latitude glaciers are natural archives, well suited for studying past environmental and climatic conditions (e.g. Cecil and others, 2004). Recent studies have focused on cold, high-alpine glaciers, where meltwater formation and percolation, which could destroy the glaciochemical signature, is negligible. In the Alps, such glaciers are found at altitudes >4000 m a.s.l. (for instance in the Monte Rosa and Mont Blanc areas; Funk, 1994). Therefore, suitable glacier archives are rare and the available paleoclimate information is spatially very limited. In order to enlarge this spatial coverage, the potential of temperate glaciers to preserve climatic records has recently been investigated. These studies suggest that, whereas trace elements seem vulnerable to meltwater percolation in the firn, stable-isotope signatures may be preserved (Eichler and others, 2000; Pohjola and others, 2002; Schotterer and others, 2004).

Subsurface ice accumulations in ice caves, some of which are located at altitudes well below the 0°C isotherm, may also have potential as paleoclimate archives (Perroux, 2001). In marked contrast to high-alpine glaciers, summer climatic conditions are assumed to have a negligible effect on the annual mass balance of cave ice (e.g. Ohata and others, 1994; Luetscher and others, 2005). Thus, the glaciochemical properties of cave ice should mainly reflect the winter temperature and precipitation regime. Such specific proxy data for the winter climate are particularly rare, as most other paleoclimate archives, such as tree rings, mainly reflect summer conditions. Preliminary glaciological investigations of cave ice have been undertaken in several European and North American ice caves (e.g. Scarisoara cave, Romania (Holmlund and others, 2005); Focul Viu ice cave, Romania (Fórizs and others, 2004); LoLc 1650, Italy (Citterio and others, 2004); Crowsnest and Canyon Creek ice caves, Canada (Yonge and MacDonald, 1999)). However, although most authors agree that low-altitude cave ice is a result of current accumulation processes, there has been only limited work on dating. Development of reliable dating methods for cave ice is essential if it is to provide a useful paleoclimate archive.

The main dating tool applied in ice-core studies is the counting of annual layers of one or more seasonally varying parameters. In addition to the visible stratigraphy, these parameters include the stable-isotope ratios $\delta^{18}O$ and δD, bulk parameters such as the dust or acidity content, and the concentration of a chemical tracer, such as NH_4^+, Ca^{2+} or NO_3^- (e.g. Eichler and others, 2000). One of the prerequisites for annual-layer counting is the preservation of seasonal accumulation of snow, but for subsurface ice accumulations this may not be the case. However, unlike glacier ice, cave ice quite frequently includes organic material (soil, vegetation, wood, etc.), which has entered the cave. Such surface-derived material may in itself provide a seasonal marker but, in addition, analysis of detrital organic material, for instance using palynology, dendrochronology or radiocarbon dating, may represent a valuable alternative approach to the determination of the ice chrono-stratigraphy. In fact, limited results from ^{14}C dating of organic material enclosed in massive subsurface ice accumulations suggest that some of these deposits may be more than 1000 years old (e.g. Schroeder, 1977; Lauriol and Clark, 1993; Achleitner, 1995; Pavuza and Spötl, 1999; Kern and others, 2004; Holmlund and others, 2005).
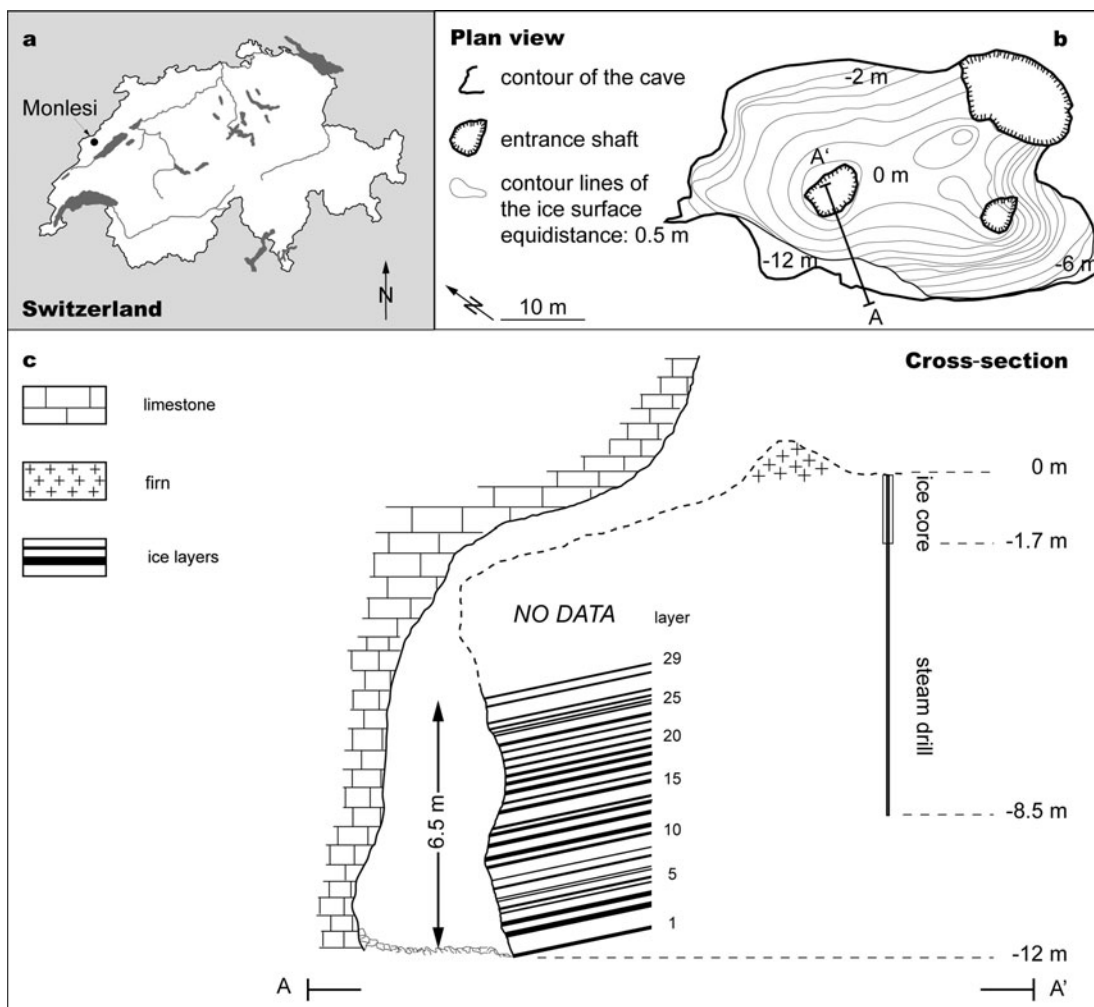
Fig. 1. (a) Map, (b) plan view and (c) cross-section of the Monlesi cave ice deposit. Although the study site is located in a region where the mean annual air temperature is 4.5°C, a 6000 m^3 subsurface ice deposit is present.

Where the conventional stratigraphic methods cannot be applied due to irregular deposition rates, radiometric methods may represent a useful alternative for the dating of ice cores. In particular, the ^{210}Pb method (half-life, $t_{1/2}$: 22.3 years) can be used for dating glacier ice on a century scale (e.g. Gäggeler and others, 1983; Von Gunten and others, 1983). Empirical estimates of the mean annual ^{210}Pb activity for several sites in Switzerland suggest that a constant ^{210}Pb activity in winter precipitation can be assumed (Schotterer and others, 1977; Von Gunten and others, 1983; Von Gunten and Moser, 1993). Additionally, tritium and ^{137}Cs peaks, associated with atmospheric nuclear tests and the Chernobyl accident, respectively, represent useful stratigraphic markers for the dating of ice cores (e.g. Eichler and others, 2000). With a detection limit of 1 TU (0.118 Bq kg^{-1}), ^{3}H should still be detectable in 50 year old ice ($t_{1/2}$: 12.3 years; Lucas and Unterweger, 2000). This is especially true for the 1963 peak, where ^{3}H activity in precipitation reached nearly 700 Bq kg^{-1} (cf. ∼60 Bq kg^{-1} in 2006) (Clark and Fritz, 1997).

This study aims to test several methods, routinely applied to the dating of alpine ice cores, for the dating of cave ice in Monlesi ice cave, Swiss Jura Mountains. These methods include stratigraphic observations, measurements of the mass turnover rate and analyses of ^{14}C, δ^{18}O, ^{137}Cs, ^{3}H and ^{210}Pb.

STUDY SITE AND METHODS

Study site

The Jura Mountains form an arc, ∼400 km wide, between the Savoie, France, in the southwest and the Black Forest, Germany, in the northeast. The inner part of this range, mostly located in Switzerland, is characterized by a succession of ridges and valleys ranging between 1000 and 1500 m a.s.l., with the highest peaks reaching about 1700 m a.s.l. Mean annual air temperature measured at these altitudes is between 6.5 and 3.5°C. The maximum annual range in daily temperature can be as high as 50°C, while a difference of 17°C between the warmest and the coldest months is common. Owing to the westerly wind regime, the Jura Mountains have abundant precipitation, usually 1200–1600 mm a^{-1}, with more than 2000 mm a^{-1} on the highest ridges. Snow occurs on ∼50 days a^{-1} and represents half of the total precipitation. Although this mountain range does not belong to previously recognized permafrost areas (Keller and others, 1998), there are 25 caves with perennial ice deposits (Luetscher and others, 2005).

Monlesi glacier (46°56′18″ N, 6°35′4″ E, 1135 m a.s.l.; Fig. 1) was selected for this study because it contains a large ice body with visible ice stratification. The cave has three entrance shafts leading, at 20 m below surface, to a large room 15 m high and 20 m × 40 m in area, which is mostly

filled with ice. The ice body is convex, with a maximum thickness of 12–15 m and a volume of 6000 m^3, though there remains uncertainty as to the exact geometry at the base of the ice (Luetscher, 2005). From cave air temperature records, Luetscher and Jeannin (2004b) demonstrate that the cave is a thermal cold trap. During the winter season (November to April) when outside air temperatures are negative, there is a good correlation between temperatures inside and outside the cave, although a buffering of the signal is observed due to heat exchanges within the cave. Conversely, from May to October, the cave shows a very stable temperature close to 0°C, which is controlled by the phase changes of the melting of ice. The average cave air temperature measured during the complete 2002/03 annual cycle was –0.7°C.

Cave ice types and accumulation processes

Two major types of ice deposit are generally recognized in ice caves: firn and congelation ice (Luetscher and Jeannin, 2004a). Firn ice results from the regelation of snow accumulated at the base of the cave entrance during the winter season. In contrast, congelation ice develops preferentially during spring, when exterior snowmelt and precipitation result in infiltration of water which refreezes in the cave. During the winter the ground is mostly frozen and percolation is significantly reduced. Although chemical differentiation between firn ice and congelation ice is possible, based on the content of dissolved carbonate (e.g. Shumskii, 1964), distinguishing between the types relies mostly on the appearance of the ice. Firn ice has an isotropic structure comprising of coarse equidimensional grains, and thus tends to be opaque and reflective. Firn layers are mostly parallel to the cave substratum and are assumed to represent seasonal deposits that are often interpreted as annual. Congelation ice consists of centimeter-sized orientated ice crystals attributed to individual freezing events. Congelation ice is easily recognizable in situ, because of its transparency and strong absorption of light. It is often associated with a thin deposit of cryogenic cave calcite formed by the segregation of solutes during freezing. Where layers are present in congelation ice, they may represent shorter periods of active ice accumulation, for instance associated with specific recharge events/snowmelt. However, after deposition, both firn and congelation ice may be subject to summer season ablation, and the accumulation of detrital material from the cave roof or transported from the exterior may form prominent annual marker layers. But complex stratigraphic sequences may also be formed, causing difficulties in the identification of individual ice layers.

The counting of visible layers may permit dating of cave ice if the ice is actively accumulating or the age at the top of the sequence is known, and the layers are annual. However, net annual ice accumulation ($\Delta m_{accumulation}$) results from the difference between the seasonal deposition of cave ice ($m_{deposited}$) and its ablation ($m_{ablated}$):

$$\Delta m_{accumulation} = \int_{year} \left(m_{deposited} - m_{ablated} \right) dt. \quad (1)$$

When $m_{deposited} \leq m_{ablated}$, no annual ice layer is preserved and debris layers may coalesce. Thus, the visible layering may underestimate the age of the cave ice because of the amalgamation of individual annual layers.

Mass turnover rates

While the formation of new cave ice commonly occurs at the top of the ice deposit (either by the crystallization of congelation ice or the formation of firn), ablation may occur from all surfaces of the ice body including the top, sides and base. At ice–air interfaces, the rate of ablation is determined by the supply of heat by air convection or water percolation. In contrast, at the ice–rock (basal) interface, melting occurs due to conduction of heat from the underlying bedrock. Although it is beyond the scope of this paper to quantify the heat transfers which control the mass balance of cave ice, the high heat capacity of the bedrock walls causes essentially constant boundary conditions, with the temperature at the cave walls close to the external mean annual air temperature at the same altitude (Luetscher and Jeannin, 2004c). A constant heat flux can therefore be assumed at the ice–rock interface, suggesting a constant rate of melting of the basal cave ice. Thus, overall, the mass balance (ΔM_{ice}) of subsurface ice deposits is a result of the difference between long-term annual ice accumulation (Equation (1)) and basal melting at the ice–rock interface:

$$\Delta M_{ice} = \int_{time} \left(m_{deposited} - m_{ablated} \right)_{surface} - \left(m_{ablated} \right)_{base} dt. \quad (2)$$

For an equilibrium ice mass, long-term surface net accumulation must equal the ablation due to basal melting ($(m_{ablated})_{base}$). Thus, if we assume that the cave ice mass balance is at equilibrium (i.e. no major fluctuations in the ice thickness), then by measuring the rate of lowering of the ice layers in a vertical section, an estimate of age (A) of the basal layers can be obtained from the total ice thickness (d):

$$A = \frac{d}{(m_{ablated})_{base}}. \quad (3)$$

EXPERIMENTAL
Field measurements

Due to the narrowness of several of the cave passages, a topometric survey of the cave was conducted using a sighting compass and clinometer (Suunto Precision Instruments; accuracy ± 1 gon ($= 1$ grad $= \pi/200$)) and a Leica laser distance meter (accuracy ± 2 mm). Accuracy was improved by systematic back- and foresight measurements, the overall accuracy in plan and vertical position is estimated as ± 5 cm. The annual ice mass accumulation ($\Delta m_{accumulation}$) was determined manually by measuring the distance between reference points fixed on the rock and the ice surface (± 5 mm). The rate of lowering of the cave ice body ($(m_{ablated})_{base}$) was determined from the position of three metal rods fixed 20 cm deep into the vertical surface of the ice body. The position of the rods was measured at irregular time intervals between 2001 and 2006, allowing an average long-term (multi-annual) rate of lowering to be determined.

Initially a steam Heucke ice drill was used to try to determine the total ice thickness in the cave. However, the presence of abundant clastic sediment limited these soundings, and only the upper 8.5 m of cave ice was penetrated. The borehole was equipped on 22 March 2002 with five Pt100 thermistors previously calibrated with a reference thermometer (Swiss Metrology Office; precision ± 0.03°C).

The thermistors were placed above the ice and at depths of 1, 2, 4 and 8 m below the ice surface, the borehole refreezing the day after drilling. In order to assess heat exchange at the rock–ice interface, the ice temperatures were monitored in this borehole from November 2002 to November 2003 at 30 min intervals. However, due to failure of the monitoring device, a gap in the record is present between 9 August and 25 September 2003.

Sampling

A small, lightweight coring system, FELICS (fast electromechanical lightweight ice-coring system; Ginot and others, 2002), was used to try to recover a complete ice core, but this proved to be difficult as ice temperatures were close to melting point, and again due to the presence of clastic sediments. Nevertheless, ice chips with a volume of a few cubic centimeters were sampled down to 1.7 m depth. Some ice-chip samples were composed of clear ice while others contained sediments and organic debris. Fifteen additional ice samples were collected manually from the accessible part of the ice face at depths equivalent to 5.5–12 m from the ice top using a cordless hammer drill equipped with a hole saw. To avoid possible contamination by meltwater on the ice surface, the outermost few centimeters were removed before sampling. The ice samples (diameter 8 cm, length 5 cm) were packed into polyethylene tubes and transported, cooled with dry ice, to a cold room kept at $-25°C$.

Water samples for the analysis of ^{222}Rn were collected manually at the main water inlets to the cave. Data were also acquired from the nearby Swiss National Network for the Observation of Isotopes in the Water Cycle (NISOT) precipitation station La Brévine, Neuchâtel, where tritium, $\delta^{18}O$ and δD have been measured in monthly composite samples since 1994 (Schürch and others, 2003).

Analytical procedures

Carbon-14 analyses were performed at the accelerator mass spectrometry (AMS) laboratory of ETH-Zürich by measuring the $^{14}C/^{12}C$ ratio. Wood samples were pretreated in a Soxhlet apparatus, using hexane, acetone and ethanol, followed by the standard acid–alkali–acid treatment. The procedure described by Vogel and others (1984) was used for graphitization. Calibration of the ^{14}C ages was performed using the program CalibETH (Niklaus and others, 1992).

Analyses of $\delta^{18}O$ in the cave ice were carried out at the Paul Scherrer Institute, Villigen, Switzerland, by pyrolysis of the liquid sample at $1450°C$ in a glassy carbon reactor to produce carbon monoxide. The $C^{18}O/C^{16}O$ ratio of the gas was measured using an isotope ratio mass spectrometer (Delta Plus XL, Finnigan MAT; analytical error 0.2‰) in relation to a known reference gas. Results are reported relative to Vienna Standard Mean Ocean Water (V-SMOW; Baertschi, 1976):

$$\delta^{18}O[‰] = \left[\left(R_{sample} - R_{standard} \right) \times 1000 / R_{standard} \right], \quad (4)$$

where, R is the ratio $^{18}O/^{16}O$ and $R_{standard} = (2005.20 \pm 0.45) \times 10^{-6}$.

The tritium content of ice was determined, using 10 mL samples, by direct β^- measurement in a liquid-scintillation spectrometer (Schotterer and others, 1998) at the Physics Institute, University of Bern. The detection limit expressed as 2σ (σ = standard deviation) is 1.6 TU.

The ^{210}Pb activity of ice was indirectly determined on 200 mL samples by measurement of the activity of the granddaughter nuclide, ^{210}Po. The ^{210}Po activity was determined after electrolytic deposition onto Ag plates by α spectrometry at an energy of 5.3 MeV (Gäggeler and others, 1983).

Radon was determined in 20 mL water samples by liquid-scintillation counting (Canberra Packard Tri-Carb 2250CA, Center of Hydrogeology, University of Neuchâtel (CHYN), laboratory). Radon in cave air samples, collected by passing $\sim$2 L of air through 180 mL Lucas cells, was measured by scintillation counting (RDA-200, Scintrex) at the CHYN laboratory. ^{238}U, ^{226}Rn and ^{210}Pb in samples of rock, soil and organic material were determined by γ spectrometry (HPGe well-type detector at the CHYN laboratory).

RESULTS

Characteristics of Monlesi cave ice

The filling of Monlesi ice cave consists predominantly of congelation ice formed from the repeated freezing of seepage water flowing over the ice surface. The generally slow rate of crystallization leads to segregation of solutes, forming transparent cave ice comprised of centimeter-sized hexagonal crystals growing perpendicularly to the substratum. Calcium carbonate segregated during the freezing process accumulates in thin powdery deposits at the top of the newly formed layer of ice. Local concentrations of this cryogenic calcite occur due to differential runoff at the ice surface. Centimeter- to decimeter-sized cryoclastic rock fragments, released by frost shattering, are also commonly observed at the ice surface during spring. Additionally, there are copious organic deposits on the ice surface due to the close proximity of the cave entrances. This allochthonous material is often associated with catastrophic events (e.g. small-scale landslides or falling trees) which occur during the summer/autumn season. Because this occurs after the phase of maximum crystallization of the cave ice, this material constitutes a good annual marker band. Measurements performed between 2001 and 2006 suggest a seasonal deposition rate ranging from 10 to 30 cm a^{-1} (average = 19 cm, $\sigma = 8$, $n = 5$), though a major part of this melts again during the course of the year. Assuming a constant rate of melting of the basal cave ice, the annual ablation at the ice surface was measured at 13.5 cm ($\sigma = 1.5$, $n = 6$), leading to a net accumulation rate of 5 cm a^{-1} (i.e. $\Delta m_{accumulation} = 46\,kg\,m^{-2}\,a^{-1}$, $\sigma = 85$, $n = 5$). However, between 2001 and 2006 the cave ice volume reduced by approximately 136 m^3, suggesting that ablation due to basal melting was dominant. The congelation ice has low porosity, as confirmed by field measurements ($\rho \sim 920\,kg\,m^{-3}$, mean value of five samples), but several macro-scale tension cracks are observed along the ice margin.

The stratigraphy of the cave ice is best observed in a vertical face between the ice body and the cave wall in the lowest part of the cave (Fig. 1c). Ice depths are referenced to the top of the ice body which lies 21 m below the surface. The 6.5 m high ice face observed between –5.5 and –12 m shows 29 individual clear ice layers, 5–36 cm thick, separated by darker bands rich in detrital material (Fig. 2). These include organic clasts (wood, leaves, bones, etc.), some anthropogenic material (pieces of metal, tiles, etc.) and carbonates (Fig. 3). The carbonates comprise bedrock fragments released by frost shattering of the cave walls (e.g. Pancza, 2006) and/or carbonate precipitates formed by the
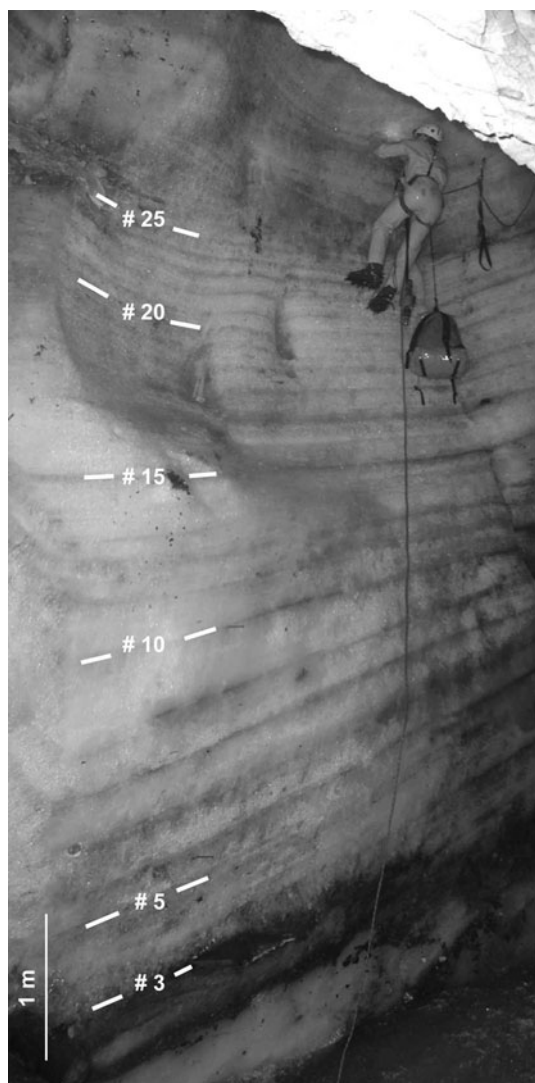
Fig. 2. View of Monlesi cave ice stratification. The presence of well-marked detrital layers (dark) is attributed to debris input associated with major melting periods (summer season).

segregation of solutes during freezing of percolating dripwater. Several of these bands are particularly visible because of their high content of insoluble particles ($>2\,g\,kg^{-1}$), and can be followed for nearly 10 m, confirming their lateral continuity. Couplets formed by clear ice layers and bands rich in detrital material show an average thickness of 18 cm ($\sigma = 8\,cm$). On this basis, between 46 and 120 individual ice couplets (1σ range) may be present for the full thickness of the ice deposit. Assuming that these couplets are annual, this indicates a maximum age of the basal cave ice at –12 m of 120 years.

Dating of detrital material

Recent studies suggest that cryogenic cave calcite can sometimes be dated by U-series (Žák and others, 2004) or ^{14}C (Lauriol and Clark, 1993). At Monlesi ice cave, our measurements indicate that the concentration of the fine fraction of carbonates varies between <0.02 and $>2\,g\,kg^{-1}$. However, we have not attempted U-series dating of this material because other measurements suggest the ice is too young for determination of a precise age. Instead we have used ^{14}C dating of the organic remains. A twig of a Norway

Table 1. Tritium analyses from Monlesi ice cave. The absence of any significant amount of ^3H in the lower part of the cave ice deposit (i.e. >5.5 m) suggests the cave ice is older than 50 years

Sample	Depth	^3H
	m	$Bq\,kg^{-1}$
Exterior snow		2.4 ± 0.3
2	–0.1	2.3 ± 0.3
3	–0.6	2.5 ± 0.3
4	–0.7	3.3 ± 0.3
5	–0.8	3.0 ± 0.3
6	–1	3.8 ± 0.3
7	–5.5	0.4 ± 0.3
8	–5.8	0.2 ± 0.3
10	–6.5	0.1 ± 0.2
11	–6.8	0.1 ± 0.2
12	–7.2	0.2 ± 0.3
13	–7.6	0.6 ± 0.3
14	–8.5	0.4 ± 0.3
17	–10	0.2 ± 0.3
19	–10.6	0.0 ± 0.3
20	–11.6	0.3 ± 0.3

spruce (*Picea abies* (L.) Karst.), sampled in the lowest ice layer at –12 m, provided an AMS ^{14}C age of 230 ± 45 years. The temporal variation of ^{14}C production during the last 100 years does not allow determination of an accurate age, but age calibration suggests the sample has a 2σ range of AD 1517–1950. The upper age limit was confirmed by the presence in the ice, at –10 m depth (layer No. 9), of a tile manufactured between 1874 and 1916 (personal communication from B. Boschung, 2002), which suggests a maximum age of ice in layer No. 10 of 132 years. Similarly, a candle and a nail buried in the cave ice at –5.5 m depth (layer No. 29) are attributed to early speleological explorations of Monlesi ice cave which started in 1954. Given the respective positions of the observed artefacts, a maximum age ranging between 109 and 158 years is obtained for the basal cave ice (i.e. layer No. 1).

Dating by determining mass turnover rates

Ice temperatures recorded in the borehole in Monlesi cave ice from November 2002 to August 2003 reveal seasonal temperature oscillations throughout the entire ice depth, with a buffering and phase shift of the signal with depth (Fig. 4). Temperatures measured at –8 m have values close to 0°C, suggesting a temperate ice body subject to melting at the rock–ice interface. This basal melting is confirmed by the observed lowering of the marker rods inserted into the ice face between 2001 and 2006 (Fig. 5). The data display a constant rate of lowering of $8 \pm 2\,cm\,a^{-1}$. Thus, given an ice thickness of 12 m and assuming an equilibrated mass balance for the cave ice, complete mass turnover is estimated to take between 120 and 200 years.

Variation of $\delta^{18}O$

Oxygen isotope analyses were performed on 58 samples taken from the Monlesi ice core 1–1.7 m below the ice surface. This is the highest sampling resolution possible given the coarse texture of the ice. Results show $\delta^{18}O$ varying between –7.3‰ and –12.3‰ (Fig. 6), although the variation is less evident between –1.05 and –1.25 m,

Depth	Stratigraphy	Layer No.	Description	Estimated age
0 m	no data		Layered congelation ice deposits separated by cryogenic calcite; numerous stones issued from frost shattering; some organic debris.	2004
-2 m				
-6 m		29	candle, nail	≥1954
		25	cryogenic calcite	
		20		
-8 m		15	cryogenic calcite, clay clay	
			clay, tile	
-10 m		10	organic material (leaves, wood), clay, tile earth, clay	tile: >1874
		5	fir needles planks, trunks, earth, metal pipe	>1850 ?
-12 m		1	organic material (leaves, wood, earth)	^{14}C: 230 ± 45 BP

Fig. 3. Stratigraphy of Monlesi cave ice. Detrital material separates annual ice layers and significantly constrains the age model of the cave ice deposit.

possibly due to isotope remobilization during phase changes. However, the oscillating signal observed between –1.3 and –1.7 m is an indication of the presence of a seasonal signal, and the mean value of –9.7‰ (σ: ±1‰) is in good agreement with δ^{18}O values in precipitation during the main period of cave ice accumulation (March to May) (Schürch and others, 2003). By attributing maxima and minima to seasons, the data suggest a mean accumulation rate ranging between 6 and 10 cm a^{-1}.

Radiometric dating of ice samples

### Tritium (^{3}H)

Two separate sets of ice samples from Monlesi cave were analyzed for tritium (Table 1). Five samples were taken from the ice core drilled in the upper layers of the ice (–0.1 to –1 m), while ten further samples were taken manually from the lower ice layers (–5.5 to –12 m). Tritium activities measured in the upper five samples have a mean of 3 Bq kg^{-1} and a range of 1.5 Bq kg^{-1}. These values are much lower than expected from precipitation affected by thermonuclear bomb testing in the 1960s, and are consistent with the tritium content of modern rainfall reported from the Brévine station of NISOT (Schürch and others, 2003). We thus assume that the upper levels (above –1 m) of the ice are modern deposits (i.e. <20 years old). Conversely, analyses of samples taken below 5.5 m depth do not show any significant ^{3}H content (Table 1). This indicates an age of more than 50 years, implying a maximum accumulation rate of 11 cm a^{-1}.

Lead-210

Figure 7 presents results of ^{210}Pb analyses performed on 14 ice samples taken at different depths in the lower ice layers (i.e. –5.5 to –12 m). The ^{210}Pb activities vary between 11 and 205 mBq kg^{-1} and are closely related to the presence of sediments within the ice samples. A composite sample of limestone from Monlesi ice cave was analyzed for U-series isotopes. The measured activity of ^{238}U was 16.9 Bq kg^{-1}, and the decay chain was in secular equilibrium. In contrast, samples of surface soils and organic debris present on the ice surface (Table 2) exhibited disequilibrium in the ^{226}Ra/^{210}Pb ratios, and high ^{226}Ra activities. The presence of ^{40}K and ^{137}Cs (mainly from the 1986 Chernobyl release; De Cort and others, 1998) suggests that this enrichment is caused by atmospheric fallout and is not produced within the cave. Finally, the radon activity measured in Monlesi drip-water during flood events (mean discharge 2.3 L min^{-1}) is ~10 Bq L^{-1} (21 samples taken for various recharge events; $\sigma = 1.8$ Bq m^{-3}), while cave air values are around 486 Bq m^{-3} (3 samples; $\sigma = 34$ Bq m^{-3}). These data suggest that there may also be a contribution to ^{210}Pb of ice from this source.

The observed activity of recent clear massive congelation ice (82.2 mBq kg^{-1}) is consistent with values expected from precipitation water. Although the analyses of clear ice samples show a small dispersion (8 samples; $\sigma = 6.4$ mBq kg^{-1}), the data display a decreasing trend with depth ($R^2 = 0.76$) which results in a mean cave ice accumulation rate of 15 cm a^{-1} (Fig. 7).
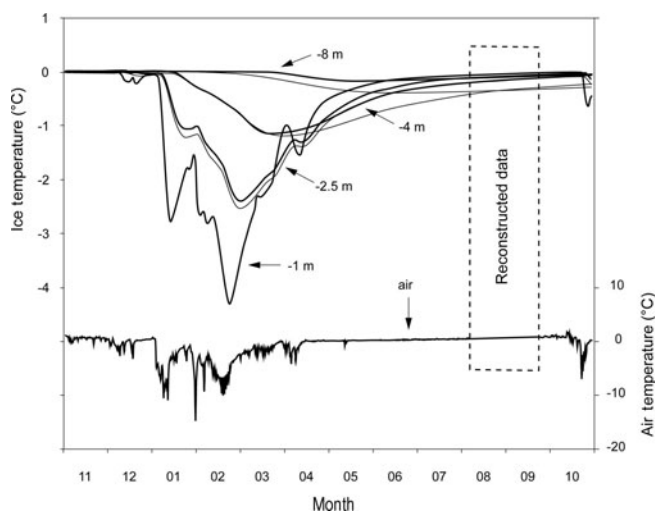
Fig. 4. Daily mean temperature recorded at different depths in the Monlesi cave ice, November 2002 to November 2003. Measured values (bold curves) fit well with a two-dimensional heat diffusion model (faint curves) assuming a constant temperature of 0°C at the ice–rock interface. Differences between the measured and modelled data are attributed to uncertainties in the geometry of the ice volume.

DISCUSSION

Our observations of ice petrography indicate that the majority of the ice in the Monlesi ice cave is congelation ice. The low permeability of this large ice mass suggests a reduced risk of remobilization due to percolating meltwater. Congelation ice develops preferentially during spring, when exterior snowmelt causes infiltration of water which refreezes in the cave. Thus, a distinctive annual banding in ice petrography is expected and observed. Layers are also clearly marked by the presence of external debris which enters through the cave entrance predominantly during the summer, after accumulation of the majority of the ice in spring. However, there appears to be considerable variation in the density of the detrital material, and not all annual layers are represented by visual bands. Conversely, some layers rich in detrital material could be due to the amalgamation of individual bands when $m_{deposited} \leq m_{ablated}$. This conclusion is well supported by a negative mass balance (M_{ice}) measured during the 2001–06 observation period. Therefore, the net accumulation rate of 5 cm a^{-1} must be considered as a minimum value, suggesting that the cave ice is younger than 240 years old. It is also worth noting that while the annually deposited cave ice ($m_{deposited}$) shows a significant dispersion
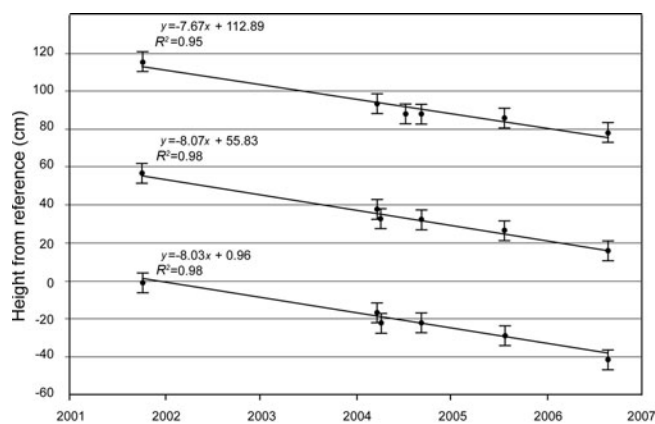
Fig. 5. Height of three reference points buried in a vertical ice outcrop in Monlesi cave. Vertical error bars represent the accuracy of field measurements (± 5 cm). The regression lines show the annual lowering of the ice mass (cm a^{-1}); the standard errors of the gradients are 3.11, 2.07 and 2.13.

($\pm 40\%$), only small variations were observed in the measured ablation rates ($m_{ablation}$, $\pm 8\%$). This result is in good agreement with previous observations, suggesting that rapid changes in the cave ice mass balance are independent of the summer climate (Luetscher and others, 2005).

Detailed laboratory measurements on a continuous core are required for precise identification of the banding. Unfortunately, we were not able to obtain a long ice core through the deposits because ice temperatures were close to melting point and the lightweight FELICS coring system was unable to drill through clastic sediments. Thus we could not apply this annual band-counting method for development of an ice chronology. Nevertheless, the oscillating signal observed for ice δ^{18}O in the upper part of the deposit, between –1.3 and –1.7 m, suggests the presence of a seasonal signal, although part of it may be lost due to remobilization during phase changes. Interpreted ice-layer thicknesses agree satisfactorily with estimates of cave ice accumulation, but the signal may be buffered by in-cave dynamic processes. Luetscher and Jeannin (2004b) concluded that sublimation is at a maximum during cold winter days, when the temperature difference between the cave air and the external atmosphere is high. Similarly, resublimation of water vapor is observed in the presence of humid air circulation. The latter process results in less negative δ^{18}O values at the top of annual ice layers. Thus, a complex stable-isotope record may be preserved in the cave ice. An analogous interpretation has been made by Yonge and

Table 2. Radioactivity of detrital material found in Monlesi ice cave. The overlying soil is the origin of most of the radioactivity observed within the cave

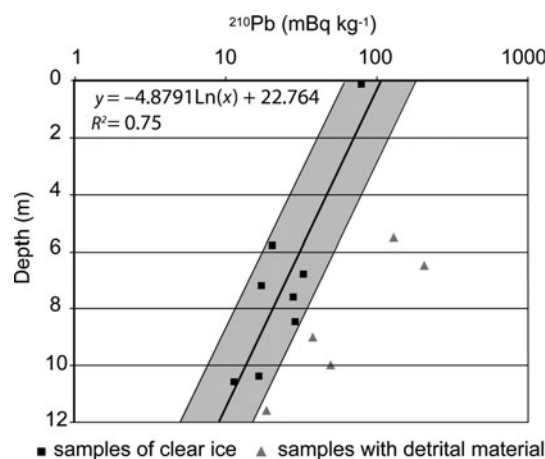| Sample	^{238}U	^{226}Ra	^{210}Pb	^{137}Cs	^{40}K
	Bq kg^{-1}	Bq kg^{-1}	Bq kg^{-1}	Bq kg^{-1}	Bq kg^{-1}
Kimmeridgian limestone (Monlesi)	16 ± 9	20 ± 33	26 ± 7	n.d.	n.d.
Reference soil sample (Marchairuz)	63 ± 13	343 ± 3	191 ± 15	n.d.	n.d.
Organo-clastic material (Monlesi)	30 ± 18	101 ± 43	386 ± 28	157 ± 30	48.5 ± 4
Cryogenic calcite (Monlesi)	20 ± 15	<40	641 ± 28	89 ± 22	21.8 ± 2

Note: n.d.: not detected.
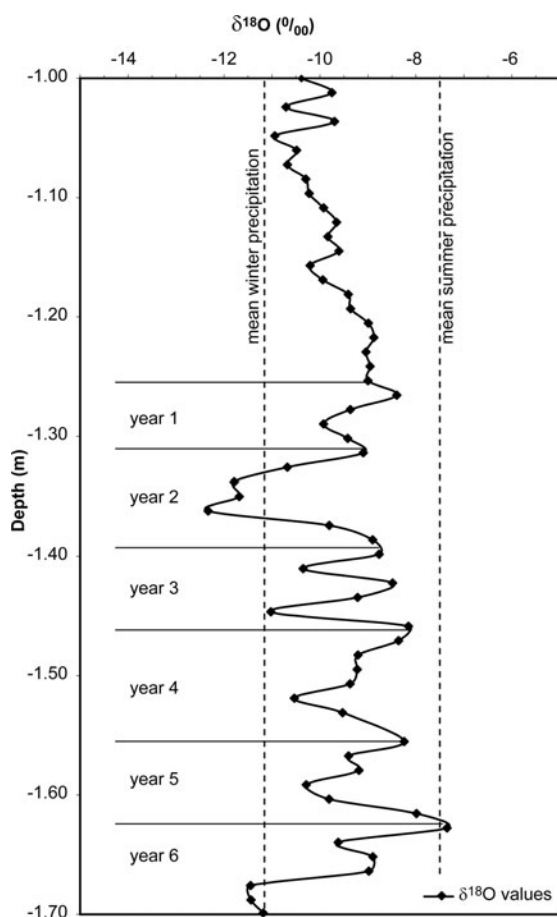
Fig. 6. Oxygen isotope data on a 70 cm long section of the Monlesi cave ice core. While part of the data in the upper section could be lost during ablation periods, the lower section of the core suggests a preserved seasonal signal. Suggested annual layers are indicated and the resulting annual accumulation rates correspond in order of magnitude to those from other methods.


Fig. 7. Lead-210 activities of ice samples from Monlesi ice cave. The decay with depth of clear ice samples is consistent with a mean accumulation rate of ~15 cm a^{-1}. The envelope (gray) represents the natural variability observed in modern precipitation. Samples containing detrital material were excluded from the relationship because they contain excess ^{210}Pb adsorbed on the sediment.

MacDonald (1999) for the isotopic composition of cave ice from Crowsnest and Canyon Creek caves in the Canadian Rocky Mountains.

It is clear from the seasonal variation of ice temperature recorded in the borehole (Fig. 4) that the Monlesi cave ice is affected by melting at the lower boundary. We have compared the thermistor temperature/depth data to predictions from a simple two-dimensional heat diffusion model. The model considers a homogeneous body with no internal heat generation. The thermal properties are those of pure ice. Boundary conditions are given by seasonal daily temperature fluctuations at the upper boundary, and an assumed constant temperature of 0°C at the lower boundary. The two-dimensional model comprises 132 cm × 12 cm cells over a depth of 15.84 m (the estimated thickness of the ice). Lateral dimensions of the model were adjusted to the known cave ice geometry with a maximum width of 10.8 m. The temperature distribution with depth is given by the Fourier equation solved numerically with an explicit finite-difference scheme (e.g. Mitchell and Griffiths, 1980), i.e.

$$\frac{\partial T}{\partial t} = a \left(\frac{\partial^2 T}{\partial x^2} + \frac{\partial^2 T}{\partial y^2} \right), \tag{5}$$

where T is temperature, t is time, a is thermal diffusivity of ice (1×10^{-6} m^2 s^{-1}), x is horizontal dimension and y is vertical dimension.

The measured data are in good agreement with the heat diffusion model of the cave ice, considering the uncertainty in the geometry of the ice body. Temperatures measured at −2.5 m almost perfectly match the modelled values. The model suggests that the temperature distribution in the upper section of the ice body is dominated by one-dimensional heat diffusion. However, there is a significant discrepancy between observed and modelled data with increasing depth. This is reflected mainly in lower observed temperature amplitudes than predicted, and is attributed both to uncertainties in the geometry of the ice volume and to heterogeneities in the ice mass (e.g. cracks). Nevertheless, borehole temperatures in Monlesi cave ice confirm the presence of a temperate ice mass and therefore support the basal melting model.

The topometric data indicate a rate of basal melting of ~8 cm a^{-1}. This value is higher than the average accumulation rate measured between 2001 and 2006 and thus explains the observed negative mass balance of the cave ice. The resulting geothermal heat flux, ~0.8 W m^{-2}, is in good agreement with estimates from rock temperature measurements performed in four different boreholes drilled within the cave walls (Luetscher, 2005). Given an ice thickness of ~12 m, complete mass turnover must, on average, occur after ~150 years (Fig. 5). This agrees with the presence of a tile manufactured between 1874 and 1916, which was located within the ice at 10 m depth, and suggested a maximum age of 158 years for the basal ice layer. Given variations in ^{14}C production in the atmosphere, the AMS ^{14}C age of 230 ± 45 years for a twig recovered from the ice at 12 m depth is unable to further constrain the age of the deposits, age calibration suggesting that the sample has a 2σ probability of being less than 500 years old.

Although recent investigations considered superficial contamination as a critical factor for the reliability of tritium analyses in cave ice (e.g. Pavuza and Mais, 1999; Pavuza and Spötl, 1999), our tritium data confirm that the lower (<−5.5 m) part of the ice is >50 years old. In relation to dating by the ^{210}Pb method, recent clear massive congelation ice has a ^{210}Pb activity consistent with values expected from modern precipitation (e.g. Schuler and others, 1991).
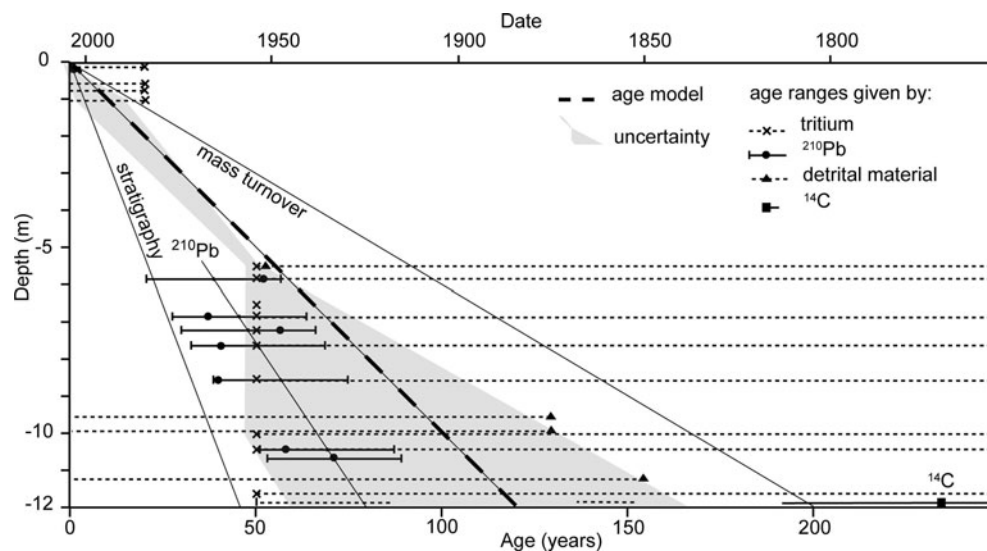
Fig. 8. Age model of the subsurface ice accumulation in Monlesi ice cave. The synthesis of different methods applied for the dating of the Monlesi cave ice suggests an age of 120 years for the lower ice layers. The gray envelope illustrates the uncertainty of this model.

A general decrease of ^{210}Pb is observed with depth, but elevated ^{210}Pb activities are recorded from some ice samples which contain debris. These high values are primarily attributed to the adsorption of ^{210}Pb after melting of the superficial cave ice, but part of this contamination could also originate from the detrital material itself. Therefore, additional sources of ^{210}Pb must be considered. While the ^{238}U content of the local limestone is too small to represent a significant input, exterior soil samples show high enrichment of ^{226}Ra (Table 2). This ^{226}Ra is adsorbed by the humic, amorphous and oxidic fractions of the soil materials including ferrihydrites and goethite (Von Gunten and others, 1996). Thus, leaching of the soil cover during precipitation events or snowmelt could lead to increased concentration of the decay product, ^{210}Pb, in subsurface drainage (Surbeck and Medici, 1991; Von Gunten and others, 1996). Furthermore, if we assume that cave ice results only from the refreezing of infiltration water, the rate of ^{210}Pb input from dissolved ^{222}Rn can be assessed using

$$[^{210}\text{Pb}] = \{(t_{1/2}{}^{222}\text{Rn})/(t_{1/2}{}^{210}\text{Pb})\} * [^{222}\text{Rn}], \quad (6)$$

where $[^{210}\text{Pb}]$ is the specific activity of lead-210, $t_{1/2}{}^{222}\text{Rn}$ is the half-life of radon-222, $t_{1/2}{}^{210}\text{Pb}$ is the half-life of lead-210 and $[^{222}\text{Rn}]$ is the specific activity of radon-222.

From Equation (6) and the ^{222}Rn activity of ~10 Bq L^{-1} measured for Monlesi seepage water, the potential contribution from this source represents only a few percent of the ^{210}Pb input from precipitation. Contamination could also occur via dry ^{210}Pb deposition from decay of ^{222}Rn, which is enriched in the cave atmosphere. The 'volume traps' approach of Oberstedt and Vanmarcke (1996) and Falk and others (2001) provides an empirical relation between the ^{222}Rn activity in the atmosphere and ^{210}Pb deposition:

$$[^{222}\text{Rn}]/[^{210}\text{Pb}] = 42, \quad (7)$$

where the specific activities of radon-222 and lead-210 are given in Bq m^{-3}.

Assuming a mean ^{222}Rn activity of 500 Bq m^{-3} in the subsurface atmosphere of Monlesi ice cave, and also that ^{210}Pb deposition from the cave air is possible for only about 7 months each year (because of melting during the remaining

time), then Equation (7) indicates the mean annual ^{210}Pb enrichment of the ice is ~7 Bq m^{-2}. This value is very small compared to the natural ^{210}Pb activity of precipitation, but the balance might be inverted in caves with higher ^{222}Rn activities (e.g. Luetscher, 2005). This is especially true if ice accumulation rates are low ($\leq$100 kg m^{-2} a^{-1}). In this situation, the contribution of ^{222}Rn-enriched water circulating at the ice surface should also be considered.

It is clear that the contribution of ^{226}Ra from soil-derived debris prevents the application of the ^{210}Pb method for dating ice samples with a high content of clastic sediments. However, if we assume a value of 120 $\pm$ 60 mBq kg^{-1} for the ^{210}Pb activity of recent clear ice, and also consider the possible input of ^{222}Rn in percolation water, then the activity of layer No. 5 at –10.6 m with ^{210}Pb = 11.2 mBq kg^{-1} suggests an age between 54 and 89 years, equivalent to a maximum age of 96 years for the basal cave ice at –12 m. This is consistent with other estimates derived in this paper, suggesting that further application of the method may be worthwhile.

Table 3 summarizes the various accumulation rates and maximum ages derived in this study, and Figure 8 provides a robust age model for the subsurface ice accumulation in Monlesi cave. From the age constraints given by the different methods applied during this study, the oldest (basal layer No. 1) cave ice is considered to be 120 years old, with an estimated error of about 56 years. Although the uncertainty remains relatively high, the data clearly demonstrate the rapidity of the ice mass turnover. This finding is in marked contrast to results from other sites such as Scarisoara ice cave (Holmlund and others, 2005) and Focul Viu ice cave (Kern and others, 2004), where ancient ice (1010 $\pm$ 64 years BP and 1230 $\pm$ 40 years BP, respectively) is present. The difference is mainly attributed to site-specific drainage patterns around the cave ice. For instance, in Scarisoara cave a highly permeable scree at the base of the ice deposit fosters the advection of cold cave air and thus reduces heat exchange with the underlying limestone. Conversely, at Monlesi a good connection with the surrounding karst system increases conductive heat transfers, and thus increases the mass turnover rate.

CONCLUSIONS

The time-span of mid-latitude subsurface ice archives is poorly known. In this case study, conducted in the Monlesi ice cave, we investigate the accuracy and limitations of several dating methods. Our results suggest that dating is possible if a multi-parameter approach involving isotopic tracers and stratigraphic markers is adopted. Ice petrography, debris content and oxygen isotope composition have the potential for identification of annual growth layers. The counting of visible ice layers could, however, be misleading as there may be hiatuses due to negative accumulation rates for individual years. We were unable to recover a continuous core from the Monlesi ice cave deposits, limiting application of this approach. Use of ^{3}H content of the ice and ^{14}C dating of organic debris present in the ice were also of limited utility, providing rather broad ranges for the actual age. There is, however, potential for the dating of specific 'marker' layers in massive congelation cave ice, such as the 1963 ^{3}H-peak, or ^{137}Cs from the Chernobyl accident (the latter identified in surface soil and organic debris present within the ice).

Application of the ^{210}Pb method, which has been used successfully to date glacier ice, was here confounded by the significant contributions of ^{210}Pb associated with soil and organic debris in the ice. However, dating based on ^{210}Pb activity in clear ice samples only gave results comparable to those from other methods. Further application is thus warranted. The most reliable techniques applied in our study were the determination of ice turnover rates from survey, and the dating of anthropogenic inclusions (a roof tile) in the ice. The latter method does, of course, depend on the random incorporation and recovery of such datable artefacts, while the former method requires long-term observations at accessible cross-sections in the ice volume. Furthermore, where rates of mass turnover are low, the displacement induced by basal melting may be too small to be accurately observed.

We have shown that a chronology can be established for recent cave ice deposits even when it has not been possible to obtain a continuous core. Contrary to results from other studies (e.g. Kern and others, 2004; Holmlund and others, 2005), this result implies a fast mass turnover rate for the cave ice, here induced by a heat flux of nearly 0.8 W m^{-2} at the rock–ice interface. Our study thus supports the idea that subsurface ice accumulations in temperate regions result from current processes rather than being relicts from a former glacial period. This finding also suggests that the mass balance of such cave ice must react strongly to short-term climatic changes. Further documentation of this archive is thus of some interest, and recovery of continuous ice cores which will facilitate the dating of individual ice layers with high resolution is a key priority.

ACKNOWLEDGEMENTS

Table 3. Cave ice accumulation rates in Monlesi ice cave derived using the different methods

Method	Accumulation rate cm a^{-1}
Observations at ice surface	5 ± 9
Ice stratigraphy	18 ± 8
Detrital material	7–11
Mass turnover	8 ± 2
δ^{18}O	6–10
Tritium	<11
^{210}Pb	15

REFERENCES

Achleitner, A. 1995. Zum Alter des Höhleneises in der Eisgruben-Eishöhle im Sarstein (Oberösterreich). *Die Höhle,* **46**(1), 1–5.

Baertschi, P. 1976. Absolute ^{18}O content of standard mean ocean water. *Earth Planet. Sci. Lett.,* **31**(3), 341–344.

Cecil, L.D., J.R. Green and L.G. Thompson. 2004. *Earth paleoenvironments: records preserved in mid- and low-latitude glaciers.* Dordrecht, etc., Kluwer Academic Publishers.

Citterio, M., S. Turri, A. Bini and V. Maggi. 2004. Observed trends in the chemical composition, δ^{18}O and crystal sizes vs. depth in the first ice core from the LoLc 1650 ''Abisso sul Margine dell'Alto Bregai'' ice cave (Lecco, Italy). *Theor. Appl. Karstol.,* **17**, 45–50.

Clark, I.D. and P. Fritz. 1997. *Environmental isotopes in hydrogeology.* New York, Lewis Publishers.

De Cort, M. *and 16 others.* 1998. *The atlas of caesium deposition on Europe after the Chernobyl accident.* Luxembourg, Office for Official Publications of the European Communities. (EUR Report 16733.)

Eichler, A. *and 7 others.* 2000. Glaciochemical dating of an ice core from upper Grenzgletscher (4200 m a.s.l.). *J. Glaciol.,* **46**(154), 507–515.

Falk, R., K. Almrén and I. Östergren. 2001. Experience from retrospective radon exposure estimations for individuals in a radon epidemiological study using solid-state nuclear track detectors. *Sci. Total Environ.,* **272**(1–3), 61–66.

Fórizs, I., Z. Kern, Z. Szántó, B. Nagy, L. Palcsu and M. Molnár. 2004. Environmental isotopes study on perennial ice in the Focul Viu ice cave, Bihor Mountains, Romania. *Theor. Appl. Karstol.,* **17**, 61–69.

Funk, M. 1994. Possible alpine ice-core drilling sites: an overview. *In* Haeberli, W. and B. Stauffer, *eds. Proceedings of the ESF/EPC Workshop on Greenhouse Gases, Isotopes and Trace Elements in Glaciers as Climate Evidence for Holocene.* Zürich, VAW Arbeitsheft, 40–44.

Gäggeler, H., H.R. von Gunten, E. Rössler, H. Oeschger and U. Schotterer. 1983. ^{210}Pb-dating of cold Alpine firn/ice cores from Colle Gnifetti, Switzerland. *J. Glaciol.,* **29**(101), 165–177.

Ginot, P., F. Stampfli, D. Stampfli, M. Schwikowski and H.W. Gäggeler. 2002. FELICS, a new ice core drilling system for high-altitude glaciers. *Mem. Nat. Inst. Polar Res., Special Issue,* **56**, 38–48.

Holmlund, P. *and 6 others.* 2005. Assessing the palaeoclimate potential of cave glaciers: the example of the Scäriéoara ice cave (Romania). *Geogr. Ann., Ser. A,* **87**(1), 193–201.

Keller, F. *and 8 others.* 1998. Permafrost map of Switzerland. *Collect. Nordicana Univ. Laval. Cent. d'Études Nord.* **57**, 557–568.

Kern, Z. *and 7 others.* 2004. Late Holocene environmental changes recorded at Ghețarul de la Focul Viu, Bihor Mountains, Romania. *Theor. Appl. Karstol.,* **17**, 51–60.

Lauriol, B. and I.D. Clark. 1993. An approach to determine the origin and age of massive ice blockages in two arctic caves. *Permafrost Periglac. Process,* **4**(1), 77–85.

Lucas, L.L. and M.P. Unterweger. 2000. Comprehensive review and critical evaluation of the half-life of tritium. *J. Res. Natl. Inst. Standards Technol.,* **105**(4), 541–549.

Luetscher, M. 2005. Processes in ice caves and their significance for paleoenvironmental reconstructions. (PhD thesis, Swiss Institute for Speleology and Karst Studies.)

Luetscher, M. and P.-Y. Jeannin. 2004a. A process-based classification of mid-latitude, low-altitude ice caves. *Theor. Appl. Karstol.,* **17**, 5–10.

Luetscher, M. and P.-Y. Jeannin. 2004b. The role of winter air circulations for the presence of subsurface ice accumulations: an example from Monlési ice cave (Switzerland). *Theor. Appl. Karstol.,* **17**, 19–25.

Luetscher, M. and P.-Y. Jeannin. 2004c. Temperature distribution in karst systems: the role of air and water fluxes. *Terra Nova,* **16**(6), 344–350.

Luetscher, M., P.-Y. Jeannin and W. Haeberli. 2005. Ice caves as an indicator of winter climate evolution: a case study from the Jura Mountains. *Holocene,* **15**(7), 982–993.

Mitchell, A.R. and D.R. Griffiths. 1980. *The finite difference method in partial differential equations.* Chichester, etc., John Wiley and Sons.

Niklaus, T.R., G. Bonani, M. Simonius, M. Suter and W. Wölfli. 1992. CalibETH: an interactive computer program for the calibration of radiocarbon dates. *Radiocarbon,* **34**(3), 483–492.

Oberstedt, S. and H. Vanmarcke. 1996. Volume traps – a new retrospective radon monitor. *Health Phys.,* **70**(2), 222–226.

Ohata, T., T. Furukawa and K. Osada. 1994. Glacioclimatological study of perennial ice in the Fuji ice cave, Japan. Part 2: Interannual variation and relation to climate. *Arct. Alp. Res.,* **26**(3), 238–244.

Pancza, A. 2006. La gélivation des parois rocheuses dans une glacière du Jura Neuchâtelois. *Permafrost Periglac. Process,* **3**(1), 49–54.

Pavuza, R. and K. Mais. 1999. Aktuelle höhlenklimatische Aspekte der Dachstein-Rieseneishöhle. *Die Höhle,* **3**, 126–140.

Pavuza, R. and C. Spötl. 1999. Neue Forschungsergebnisse aus der Hundalm-Eishöhle. *Landesver. Höhlenkunde Tirol,* **38**(51), 3–10.

Perroux, A.-S. 2001. Etude du fonctionnnement d'une cavité englacée durant un cycle climatique. Site de la glacière d'Autrans (Vercors). Premiers résultats. *Karstologia,* **37**(1), 41–46.

Pohjola, V. *and 7 others.* 2002. Effect of periodic melting on geochemical and isotopic signals in an ice core on Lomonosovfonna, Svalbard. *J. Geophys. Res.,* **107**(D4), 4036. (10.1029/2000JD000149.)

Schotterer, U. *and 7 others.* 1977. Isotope measurements on firn and ice cores from alpine glaciers. *IAHS Publ.* 118 (Symposium at Grenoble 1975 – *Isotopes and Impurities in Snow and Ice*), 232–236.

Schotterer, U., P. Schwarz and V. Rajner. 1998. From pre-bomb levels to industrial times. A complete tritium record from an Alpine ice core and its relevance for environmental studies. *In Isotope techniques in the study of environmental change: Prcoeedings of an International Symposium, 14–18 April 1997, Vienna.* Vienna, International Atomic Energy Agency, 581–590.

Schotterer, U., W. Stichler and P. Ginot. 2004. The influence of post-depositional effects on ice core studies: examples from the Alps, Andes, and Altai. *In* Cecil, L.D., J.R. Green and L.G. Thompson, *eds. Earth paleoenvironments: records preserved in mid- and low-latitude glaciers.* Dordrecht, etc., Kluwer, 39–59.

Schroeder, J. 1977. Les formes de glaces des grottes de la Nahanni, Territoires du Nord-Ouest, Canada. *Can. J. Earth Sci.,* **14**(2), 1179–1185.

Schuler, C. *and 10 others.* 1991. A multitracer study of radionuclides in Lake Zurich, Switzerland 1. Comparison of atmospheric and seimentary fluxes of ^{7}Be, ^{10}Be, ^{210}Pb, ^{210}Po and ^{137}Cs. *J. Geophys. Res.,* **96**(C9), 17,051–17,066.

Schürch, M., R. Kozel, U. Schotterer and J.-P. Tripet. 2003. Observation of isotopes in the water cycle – the Swiss National Network. *Environ. Geol.,* **45**(1), 1–11.

Shumskii, P.A. 1964. *Principles of structural glaciology.* New York, Dover Publications.

Surbeck, H. and F. Medici. 1990. Rn-222 transport from soil to karst caves by percolating water. *Int. Assoc. Hydrogeol. Mém.* **22**(1), 348–355.

Vogel, J.S., J.R. Southon, D.E. Nelson and T.A. Brown. 1984. Performance of catalytically condensed carbon for use in accelerator mass spectrometry. *Nucl. Instrum. Meth. Phys. Res. B,* **5**(2), 289–293.

Von Gunten, H.R. and R.N. Moser. 1993. How reliable is the ^{210}Pb dating method? Old and new results from Switzerland. *J. Paleolimnol.,* **9**(2), 161–178.

Von Gunten, H.R., E. Rössler and H. Gäggeler. 1983. Dating of ice cores from Vernagtferner (Austria) with fission products and lead-210. *Z. Gletscherkd. Glazialgeol.,* **18**(1), 37–45.

Von Gunten, H.R., H. Surbeck and E. Rössler. 1996. Uranium series disequilibrium and high thorium and radium enrichments in karst formations. *Environ. Sci. Technol.,* **30**(4), 1268–1274.

Yonge, C.J. and W.D. MacDonald. 1999. The potential of perennial cave ice in isotope palaeoclimatology. *Boreas,* **28**(3), 357–362.

Žák, K., J. Urban, V. Cílek and H. Hercman. 2004. Cryogenic cave calcite from several Central European caves: age, carbon and oxygen isotopes and a genetic model. *Chemical Geol.,* **206**(1–2), 119–136.